A Novel Oxide Ion Conductor in a Doped Bi_2O_3–V_2O_5 System: Ab Initio Structure of a New Polymorph of $NaBi_3V_2O_{10}$ via Powder X-ray Diffraction†

Digamber G. Porob and T. N. Guru Row*

Solid State and Structural Chemistry Unit, Indian Institute of Science, Bangalore-560 012, India

Received June 5, 2000. Revised Manuscript Received September 8, 2000

The crystal structure of $NaBi_3V_2O_{10}$ has been determined using the ab initio approach followed by Rietveld refinement via powder X-ray diffraction. The unit cell is triclinic, space group $P\bar{1}$, with $a = 7.1964(4)$ Å, $b = 7.0367(3)$ Å, $c = 5.5139(2)$ Å, $\alpha = 84.440(3)°$, $\beta = 113.461(2)°$, $\gamma = 112.319(2)°$, and $V = 236.46(2)$ Å^3. The final refinements gave $R_p = 9.94\%$, $R_{wp} = 13.11\%$, and $R_{(I,hkl)} = 8.73\%$ for 30 parameters and 4871 data points. These results indicate that this is a polymorph different from that reported previously and represents a new class of oxide ion conductors in solid solution of the $Na_2O-Bi_2O_3-V_2O_5$ ternary system. The $(Bi_2O_2)^{2+}$ chains extend along the *c* axis with VO_4 units joining the chains along both *a* and *b* directions resulting in a hitherto unknown motif in this class of compounds. The structure hence points to a new mode for the mechanism of oxide ion conduction.

Introduction

Oxide ion conductors have been a subject of extensive study due to their potential application in fuel cells, oxygen sensors, oxygen pumps, dense membranes for oxygen separation, and catalysis. Over the past decade, many efforts have been made to develop new materials exhibiting high oxide ion mobility at ambient temperature. In addition to the improvements of the existing materials, new classes of conductors in which the structure plays an important role have been proposed. Among these, bismuth vanadate phases have demonstrated good oxide ion conductivity.[1] The high level of conductivity in these materials is normally attributed to the presence of a defect fluorite structure related to δ-Bi_2O_3 or with $(Bi_2O_2)^{2+}$ sheets interleaved with perovskite-like layers containing random oxide ion vacancies as in the Aurivillius family. The oxide ion vacancies are either intrinsic (e.g. $Bi_2V_2O_{5.5}$) or extrinsic (e.g. $Bi_2Sr_2Nb_2AlO_{11.5}$) that are introduced by doping into either the perovskite or the bismuth oxide layer.[2] The most successful oxide ion conductors are the metal-doped bismuth vanadium oxides, $Bi_2M_xV_{1-x}O_\delta$, BIMEVOX exhibiting attractive properties. These compounds belong to Aurivillius phases, $Bi_{4+y}V_{2-y}O_{11-y}$. The doped Bi_2O_3–V_2O_5 system, in particular, has been of interest to us, and we have been exploring various phases in this class of compounds to identify new structures.[3,4] A compound $NaBi_3V_2O_{10}$ was recently isolated from the BINAVOX solid solution within the $Na_2O-Bi_2O_3-V_2O_5$ ternary system,[5] and the structure was determined to be isostructural to $Pb_2Bi_2V_2O_{10}$.[6] We found that the simulated X-ray diffraction pattern of this structure does not match with the experimental one reported earlier.[5] This led us to believe that the structure reported[6] is a different polymorph of $NaBi_3V_2O_{10}$. The synthetic protocol given by Sinclair et al.[5] was thus used to synthesize $NaBi_3V_2O_{10}$, and the structure was determined ab initio using powder X-ray diffraction data. The structure established beyond doubt that a new polymorph of $NaBi_3V_2O_{10}$ (hereafter α-NBVO) is formed.

Experimental Section

$NaBi_3V_2O_{10}$ was synthesized as per the reported procedure.[5] Single crystals of this phase (α-NBVO) could not be grown because of the presence of a concomitant minor phase which forms at around 700 °C and remains until the melting point (755 °C). High-resolution X-ray powder data were collected on a STOE/STADI−P X-ray powder diffractometer with germanium monochromated Cu $K\alpha_1$ ($\lambda = 1.540\,56$ Å) radiation from a sealed-tube X-ray generator (20 kV, 25 mA) in the transmission mode using a linear PSD ($2\theta = 3-100.42°$ with a step size of 0.02° with 6 s/step exposure time) at room temperature. The sample was rotated during the data collection to minimize preferred orientation effect, if any. The program ITO12[7] in CRYSFIRE[8] package was used to index the powder pattern, which gave a triclinic cell in agreement with the earlier report.[5] The full pattern fitting and peak decomposition in the space group $P\bar{1}$ using the program EXTRA[9] gave $R_p = 11.55\%$ and

* Corrresponding author. Tel: +91-80-3092796; +91-80-3092336. Fax: +91-80-3601310. E-mail: ssctng@sscu.iisc.ernet.in.

† Communication No. 1518.

(1) Boivin, J. C.; Mairesse, G. *Chem. Mater.* **1998**, *10*, 2870 and references therein.
(2) Kendall, K. R.; Navas, C.; Thomas, J. K.; Zur Loye, H. C. *Chem. Mater.* **1996**, *8*, 642.
(3) Sooryanarayana, K. Ph.D. Thesis, Indian Institute of Science, **1998**.
(4) Sooryanarayana, K.; Guru Row T. N.; Varma K. B. R. *Mater. Res. Bull.* **1999**, *34*, 425.
(5) Sinclair, D. C.; Watson, C. J.; Howie, R. A.; Skakle, J. M. S.; Coats, A. M.; Kirk, C. A.; Lachowski, E. E.; Marr, J. *J. Mater. Chem.* **1998**, *8* (2), 281.
(6) Sinclair, D. C.; Marinou, E.; Skakle, J. M. S. *J. Mater. Chem.* **1999**, *9* (2), 2617.
(7) Visser, J. W. *J. Appl. Crystallogr.* **1969**, *2*, 89.
(8) Shirley, R. *The CRYSFIRE System for Automatic Powder Indexing*: *User's Manual*; The Lattice Press: England, 1999.

10.1021/cm000444u CCC: $19.00
Published on Web 11/01/2000

Table 1. Crystallographic Data for $NaBi_3V_2O_{10}$

data collcn range (2θ, deg)	3.00−100.42
step scan increment (2θ, deg)	0.02
step scan time (s)	6
radiation source	sealed-tube X-ray generator
radiation	Cu Kα_1
λ (Å)	1.540 56
formula	$NaBi_3V_2O_{10}$
fw	911.80
color	yellow
space group	$P\bar{1}$
profile function	pseudo-Voigt
a (Å)	7.1964(4)
b (Å)	7.0367(3)
c (Å)	5.5139(2)
α (deg)	84.440(3)
β (deg)	113.462(2)
γ (deg)	112.319(2)
V (Å^3)	236.46(2)
Z	1
no. of data points	4871
no. of contributing reflcns	492
no. of structural params	30
no. of profile params	15
expected R_{wp}[a]	12.55
R_{wp} (%)[a]	13.11
R_p (%)[a]	9.94
$R_{(I,hkl)}$ (%)	8.73

$R_{wp} = 15.80\%$ for 498 independent reflections. SIRPOW 92 was used[10] to locate the positional parameters of bismuth and vanadium atoms, which were put in the starting model for preliminary Rietveld refinement using the GSAS[11] program. To check the symmetry, the space group $P1$ was assigned and the above procedure was repeated. The heavy atoms located clearly indicated the presence of a center of symmetry. The R_p and R_{wp} values were not significantly different in the two approaches. At this stage, the occupancy of the Bi(1) atom refined to a lower value suggesting that the Na atom must be located at the same site satisfying the overall stoichiometry. A subsequent difference Fourier map revealed the positions of the remaining oxygen atoms which were used for the final Rietveld refinement using GSAS.[11]

The profile was fitted using the pseudo-Voigt function. A Chebyshev function consisting of 12 coefficients was used to define the background. Isotropic thermal parameters of all atoms were refined independently at the early stage of refinements. It was observed that the thermal parameter of all oxygens converged to approximately same values, except that of O(3), which was higher than the rest. Hence the thermal parameter of O(3) was refined separately while those of the rest of the oxygens were constrained together and refined. Since the occupancy of O(3) showed a large deviation from unity, it was also refined. The occupancies of Bi(1)/Na were constrained (to a total value of 1.0) while those of the other atoms were fixed.

Results and Discussion

It is clear that the $NaBi_3V_2O_{10}$ exists in two polymorphic forms, a disordered phase (α-NBVO) and other an ordered phase reported[6] earlier (hereafter β-NBVO). Crystallographic and experimental parameters are given in Table 1, final positional and thermal parameters are given in Table 2, and bond lengths, bond valence sums, and bond angles are given in Tables 3 and 4, respectively. The observed, difference, and calculated patterns are shown in Figure 1. The structure of $NaBi_3V_2O_{10}$ is built of $(Bi_2O_2)^{2+}$ chains extended along the c axis with the vanadium tetrahedra acting as linkers between chains (Figure 2). This structure depicts an entirely new

Table 2. Final Atomic Coordinates and Isotropic Thermal Parameters from Powder X-ray Data at 298 K for $NaBi_3V_2O_{10}$

atom	x	y	z	occ	U (Å^2)
Bi(1)	0.2930(5)	0.1208(5)	0.6098(5)	0.557(4)	0.0322(8)
Na(1)	0.2930(5)	0.1208(5)	0.6098(5)	0.443(4)	0.0322(8)
Bi(2)	0.0264(4)	0.2586(4)	−0.0552(5)	1.000	0.0322(8)
V(1)	−0.3556(13)	0.3474(13)	−0.7014(16)	1.000	0.0290(33)
O(1)	0.0458(47)	−0.0150(47)	0.8086(53)	1.000	0.0328(49)
O(2)	0.2175(39)	0.4004(39)	0.6284(45)	1.000	0.0328(49)
O(3)	0.6762(48)	0.2549(45)	0.0776(61)	0.896(32)	0.0627(153)
O(4)	0.2666(40)	−0.1698(39)	0.4445(55)	1.000	0.0328(49)
O(5)	0.3645(44)	0.2881(46)	0.2141(56)	1.000	0.0328(49)

Table 3. Bond Lengths and Bond Valence Sum[13] for $NaBi_3V_2O_{10}$

atoms[a]	bond length (Å)	bond valence
Bi(1)−O(1)	2.310(35)	0.558
Bi(1)−O(1)	2.509(23)	0.326
Bi(1)−O(2)	2.252(32)	0.652
Bi(1)−O(3)	2.825(25)	0.139
Bi(1)−O(4)	2.231(32)	0.691
Bi(1)−O(5)	2.519(32)	0.317
Na−O(1)	2.310(35)	0.254
Na−O(1)	2.509(23)	0.148
Na−O(2)	2.252(32)	0.297
Na−O(3)	2.825(25)	0.063
Na−O(4)	2.231(32)	0.315
Na−O(5)	2.519(32)	0.144
		1.952[b]
Bi(2)−O(1)	2.204(38)	0.935
Bi(2)−O(1)	2.119(30)	0.743
Bi(2)−O(2)	2.542(29)	0.298
Bi(2)−O(3)	2.882(41)	0.119
Bi(2)−O(4)	2.258(23)	0.642
Bi(2)−O(5)	2.229(28)	0.694
		3.431[c]
V(1)−O(2)	1.667(25)	1.444
V(1)−O(3)	1.565(42)	1.903
V(1)−O(4)	1.876(29)	0.821
V(1)−O(5)	1.761(32)	1.120
		5.288[c]

[a] O(1) and O(1)′ are symmetry-related oxygens. [b] The mean bond valence sum for the site containing Bi(1) and Na is calculated by considering the contribution from both atoms: mean bond valence sum = (bond valence sum of Bi1 + bond valence sum of Na)/2. [c] Bond valence sum.

Table 4. Bond Angles for $NaBi_3V_2O_{10}$

atoms[a]	bond angle (deg)	atoms[a]	bond angle (deg)
O(2)−V(1)−O(3)	115(1)	O(1)−Na(1)−O(1)′	83(1)
O(2)−V(1)−O(4)	117(1)	O(1)−Na(1)−O(2)	80(1)
O(2)−V(1)−O(5)	110(1)	O(4)−Na(1)−O(1)	73(1)
O(3)−V(1)−O(4)	95(1)	O(4)−Na(1)−O(5)	86(1)
O(3)−V(1)−O(5)	109(2)	O(1)−Na(1)−O(2)	85(1)
O(4)−V(1)−O(5)	108(1)	O(1)−Na(1)−O(5)	67(1)
O(1)−Bi(1)−O(4)	99(1)	O(2)−Na(1)−O(5)	82(1)
O(1)−Bi(1)−O(1)	83(1)	O(1)−Bi(2)−O(1)′	70(1)
O(1)−Bi(1)−O(2)	80(1)	O(1)−Bi(2)−O(2)	76(1)
O(4)−Bi(1)−O(1)	73(1)	O(1)−Bi(2)−O(4)	79(1)
O(4)−Bi(1)−O(5)	86(1)	O(1)−Bi(2)−O(5)	78(1)
O(1)−Bi(1)−O(2)	85(1)	O(1)−Bi(2)−O(5)	80(1)
O(1)−Bi(1)−O(5)	67(1)	O(4)−Bi(2)−O(1)	105(1)
O(2)−Bi(1)−O(5)	82(1)	O(4)−Bi(2)−O(2)	80(1)
O(1)−Na(1)−O(4)	99(1)	O(2)−Bi(2)−O(5)	80(1)

[a] O(1) and O(1)′ are symmetry-related oxygens.

(9) Altomare, A.; Burla, M. C.; Cascarano, G.; Giacovazzo, C.; Guagliardi, A.; Moliterni, A. G. G.; Polidori, G. *J. Appl. Crystallogr.* **1995**, *28*, 842.

(10) Altomare, A.; Burla, M. C.; Cascarano, G.; Giacovazzo, C.; Guagliardi, A.; Camalli, M.; Polidori, G. *J. Appl. Crystallogr.* **1994**, *27*, 435.

(11) Larson, A. C.; von Dreele, R. B. *Los Alamos Lab. Rep.* **1987**, *LA-UR-86−748*.

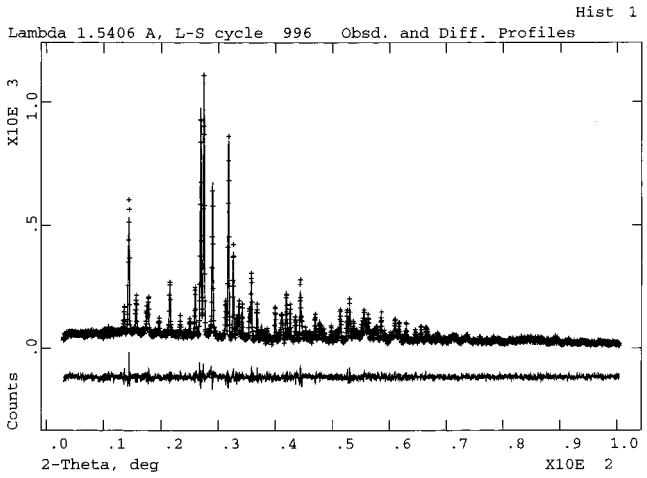

Figure 1. Observed, calculated, and difference X-ray diffraction pattern of $NaBi_3V_2O_{10}$.

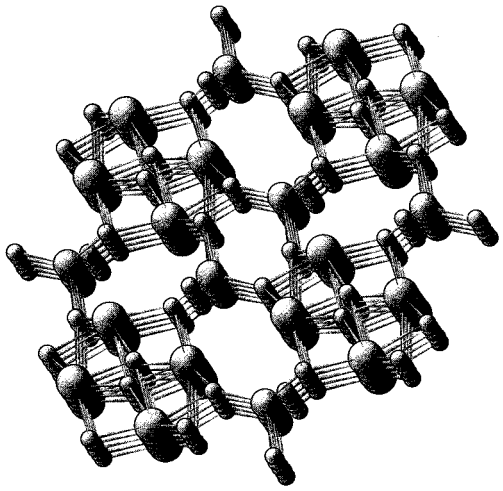

Figure 2. Structure of $NaBi_3V_2O_{10}$ viewed down the "*c*" axis.

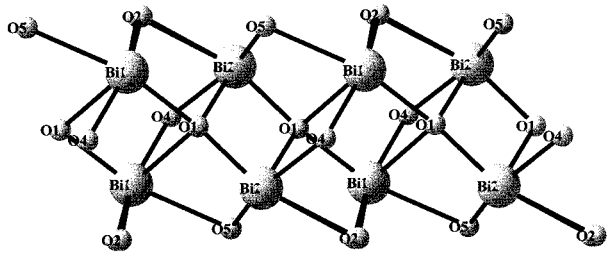

Figure 3. Buiding blocks of $(Bi_2O_2)^{2+}$ chains.

motif unlike those belonging to the Aurivillius family of compounds. It is also different from the earlier reported structure[6] of *β*-NBVO. The $(Bi_2O_2)^{2+}$ chains are made of distorted square pyramidal units of BiO_4 with Bi at the apex of the pyramid. The Bi(1) atom is bonded to O(2), O(5), and two symmetry-related oxygen's O(1) and O(1)′ while Bi(2) is similarly bonded to O(2), O(5), and two symmetry-related oxygen's O(1) and O(1)′, each forming a square pyramid. Four such square pyramidal units of BiO_4 form the basic building block of $(Bi_2O_2)^{2+}$ chains (Figure 3). The Bi−O bond lengths in $(Bi_2O_2)^{2+}$ chains vary between 2.119 and 2.509 Å. These chains are linked to one another along both *a* and *b* axes through two VO_4 units resulting in the formation of eight-membered rings (Figure 4). The V−O bond lengths vary between 1.565 (with O3) and 1.876 Å. This generates two types of ring structures running parallel to the

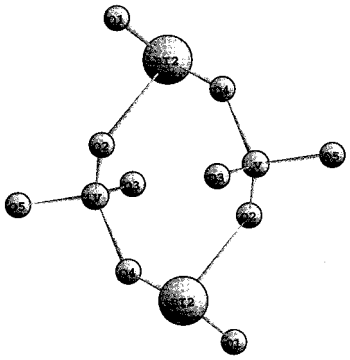

Figure 4. Perspective view of the eight-membered ring generated by $(Bi_2O_2)^{2+}$ chains and VO_4 tetrahedra.

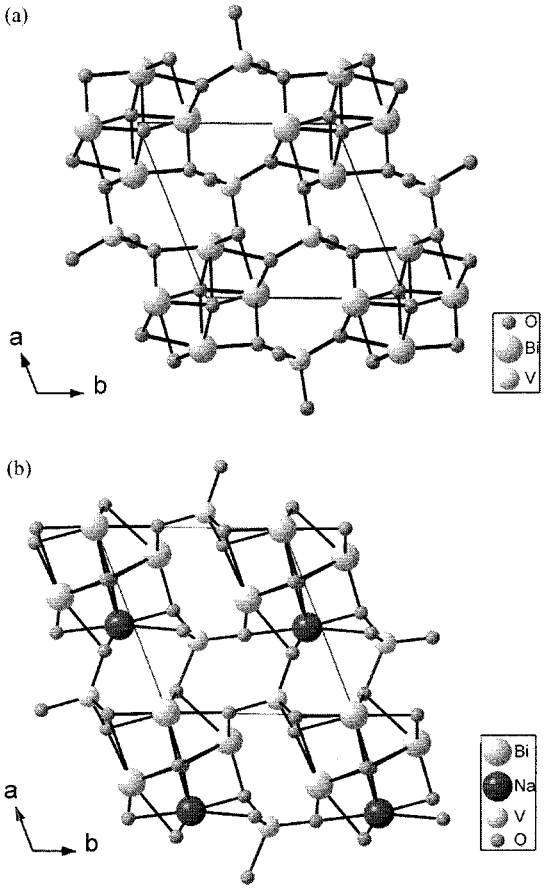

Figure 5. Comparison of the two structures of $NaBi_3V_2O_{10}$: (a) current structure; (b) reported structure from neutron data.

c axis displaying central voids with a major diameter of about 5.6 Å and minor one of about 3.6 Å (Figure 2). Similar ring structures are formed along the other two axes generating voids. This results in the formation of an extended 3-dimensional network of channels in the crystal lattice.

It is interesting to compare the structure with the *β*-NBVO polymorph,[6] which was found to be isostructural with $Pb_2Bi_2V_2O_{10}$. The *β*-NBVO structure displays cation ordering (space group *P*1) where the α-NBVO corresponds to the cation-disordered form (space group $P\bar{1}$). The bond valence sum calculations confirm the assignment of sites in this cation disordered structure (Table 3). Figure 5 shows the comparison of two crystal structures which illustrate that the bismuth coordination sphere forms "chains" in the cation-disordered form

unlike the routine layer formation in the reported structure.

The vanadium site in BIMEVOX series is known to display a dynamic disorder. The disorder of the oxygen vacancies that are associated with the vanadium atom plays an important role in ionic conductivity behavior of these compounds.[12] In the present structure, it may be noted that O(3) shows a disorder in the occupancy and thermal parameter. The V−O(3) bond protrudes into the channel formed by the eight-membered rings, and the higher thermal parameter of O(3) suggests a possible mode of ionic conductivity in this structure. Also, O(3) is above the mean plane formed by the two VO_4 bonds of adjacent rings by 0.071 Å and hence can easily get into any of these voids. The relatively longer interactions of O(3) with Bi(1)/Na and Bi(2) might have relevance in this context.

Conclusion

In conclusion, the structure of α-NBVO has been solved by the ab initio approach using powder X-ray diffraction data. The structure depicts, for the first time, features which are not common to the Aurivillius family of compounds. The usual arrangement of BiO_4 units forming $(Bi_2O_2)^{2+}$ sheets in two dimensions in the Aurivillius family is restricted to a one-dimensional chain in $NaBi_3V_2O_{10}$. The $(Bi_2O_2)^{2+}$ sheets in the doped Bi_2O_3–V_2O_5 system belonging to the Aurivillius family are known to produce an undesirable strong anisotropy in ionic conductivity. It may be speculated that the absence of these sheets in this compound might have significant impact on the conductivity behavior.

[a] $R_{wp} = (\Sigma w(I_o - I_c)^2/\Sigma[wI_o^2])^{1/2}$. $R_p = (\Sigma|I_o - I_c|/\Sigma I_c)$. $R_F = <|F_o| - |F_c|>/<|F_o|>$.

Expected $R_{wp} = R_{wp}/(\chi^2)^{1/2}\chi^2 = \Sigma w(I_o - I_c)^2/(N_{obs} - N_{var})$.

CM000444U

(12) Joubert, O.; Jouanneaux, A.; Ganne, M. *Mater. Res. Bull.* **1994**, *29*, 175.

(13) Hormillosa, C. Institute For Materials Research, McMaster University, Version 2.00, 1993.